

PeV neutrinos from wind breakouts of type II supernovae

Zhuo Li^{1,2}

¹*Department of Astronomy, School of Physics, Peking University, Beijing 100871, China;*

²*Kavli Institute for Astronomy and Astrophysics, Peking University, Beijing 100871, China*

(Dated: December 27, 2018)

Recently, the rapid multiwavelength photometry and flash spectra of supernova (SN) 2013fs imply that the progenitor stars of regular type II SNe (SNe II) might be commonly surrounded with a confined dense stellar wind ejected by themselves with large mass loss rate few years before the SNe. Based on the assumption that the pre-SN progenitor stars of SNe II have a SN 2013fs-like wind, with mass loss rate $\dot{M} \sim 3 \times 10^{-3} (v_w/100 \text{ km s}^{-1}) M_\odot \text{ yr}^{-1}$, we investigate the neutrino emission during the wind breakouts of SN shocks. We find that the regular SNe II can convert a fraction $\sim 10^{-3}$ of their bulk kinetic energy into neutrino emission, which can contribute a significant fraction of the IceCube-detected neutrino flux at $\gtrsim 300$ TeV. Moreover, the $\lesssim 200$ TeV IceCube neutrinos can be accounted for by cosmic rays produced by the shocks of all SN remnants, losing energy in their host galaxies, i.e., starburst galaxies. The future follow-up observations of neutrinos by Gen2 and gamma-rays by CTA and LHAASO from nearby individual SNe II, within weeks after the explosions, will test this model.

I. INTRODUCTION

Massive stars with initial mass larger than $8M_\odot$ end when their cores collapse. This triggers a supernova (SN), in which a strong shock is generated, propagates through the progenitor star, and ejects its envelope. The SN shock is radiation dominated inside the progenitor star, and a radiation flash is produced when the shock breakouts from the star [1]. Some observations of early SN radiation had been explained to be SN shock breakouts [e.g., 2–7]. It is predicted that the shock becomes collisionless after breakouts, and can accelerate particles, which may interact with background nucleons leading to pion and hence neutrino and gamma-ray production [8].

If the progenitor star is surrounded by a dense stellar wind the SN shock will go through this dense medium rather than the interstellar medium, and the denser medium enhance pp interaction rates and leads to more efficient pion and neutrino/gamma-ray production [9–13]. Whether there exists a dense stellar wind depends on the pre-SN evolution of massive stars, which is theoretically not well understood and difficult to observe. However, the properties of UV/optical emission and several X/gamma-ray flashes associated with SNe had suggested shock breakouts from dense stellar winds of progenitor stars [2, 3, 5, 6]. In particular, very recently it was reported that rapid follow-up photometry and spectroscopy observations of SN 2013fs map the immediate environment of the progenitor star and establish that it was surrounded by a confined, dense circumstellar material [14]. The observations indicate that SN 2013fs is a regular type II SN (SN II), thus it may be common that red supergiant stars (RSGs), progenitors of SNe II,

ejected a dense wind at a high rate just \sim yr before the SN explosions [14].

Diffuse TeV–PeV neutrinos had been first detected by IceCube [15, 16], but the origin is still unknown. IceCube did not find point sources yet for 7 yr search [17], and the Galactic, blazar and gamma-ray burst origins of the bulk diffuse neutrinos had been strongly disfavored [18–23]. The latest IceCube result from the south hemisphere [24] hints that the neutrino spectrum may not be a featureless single power law, but consist of more spectral components: the spectrum beyond a few 100’s TeV is flat $E_\nu^2 \phi_\nu \propto E_\nu^0$, consistent with the north hemisphere muon track events [24, 25], but below 100 TeV the flux is enhanced abruptly by a factor of ~ 4 [24, see Fig. 2].

Motivated by these findings, we investigate the TeV–PeV neutrino production from normal SNe II, assuming that the pre-SN progenitor stars are commonly surrounded by dense winds, up to at least $\sim 10^{15}$ cm, ejected by themselves. We find that it is likely that the wind breakouts of SN shocks can account for at least a significant fraction of the IceCube detected diffuse neutrinos at $\gtrsim 300$ TeV, and the neutrinos below ~ 200 TeV can be contributed by SN remnant (SNR) shock-produced cosmic rays (CRs) interacting with interstellar medium in the host galaxy. Note, Ref. [26] recently had calculated the neutrino flux from a SN II with SN 2013fs-like wind, but focused on the next SN in the Milky Way.

II. DYNAMICS

Consider that the pre-SN progenitor star is surrounded by a stellar wind with the density $\rho = \dot{M}/4\pi R^2 v_w \equiv AR^{-2}$, where \dot{M} is the wind mass loss rate, v_w is the wind velocity, and R is the radius. According to the measurement of SN 2013fs [14], we take $A = 1.5 \times 10^{15} A_* \text{ g cm}^{-1}$

* Corresponding author(email: zhuo.li@pku.edu.cn)

for $\dot{M} = 3 \times 10^{-3} M_{\odot} \text{yr}^{-1}$ and $v_w = 100 \text{ km s}^{-1}$, and the wind is confined but extends up to a distance of $R_w \approx 10^{15} \text{ cm}$.

The SN explosion ejects the progenitor's stellar envelope. Typically for a SN II, the total ejecta mass is $M = 10 M_{\odot}$, and the bulk kinetic energy is $E_k = 10^{51} \mathcal{E}$ erg, thus we take them as the normalization [as 27], hence the bulk velocity is $v_b = \sqrt{2E_k/M} = 3.2 \times 10^8 \mathcal{E}^{1/2} \mathcal{M}^{-1/2} \text{ cm s}^{-1}$. When the SN shock propagates down the density gradient of the outer part of the stellar envelope, it accelerates and the swept-up material is also accelerated and ejected. After the shock breaks through the stellar surface, the SN ejecta left behind has more energy for slower shell. The kinetic energy of ejecta with velocity larger than v is given by

$$E_{ej}(> v) = E_k(v/v_b)^{-\chi} \quad (v \geq v_b) \quad (1)$$

where $\chi = 3 + (5/n)$, with $n = 3/2$ and 3 for convective and radiative envelopes, respectively [27]. We take $\chi = 6$ for RSG in the following, but we also try $\chi = 5$ (for blue supergiant stars; BSGs) which gives negligible change of the results.

After acceleration in the steep gradient of the stellar outer envelope, the SN shock will be decelerated in the wind. When the shock propagates to a radius R in the wind, the total energy of the shock-swept-up wind material is $E_s = u^2 \int_0^R 4\pi r^2 \rho dr = 4\pi A R u^2$ with u the postshock fluid velocity. This shock energy is provided by the SN ejecta with velocity $v \geq u$, thus let $E_s(u) = E_{ej}(> v)|_{v=u}$, resulting in the dynamical evolution of the SN shock in the wind,

$$u = \left(\frac{E_k v_b^6}{4\pi A} \right)^{1/8} R^{-1/8}. \quad (2)$$

Note this description is available for early stage when the SN shock propagates in the wind where $u > v_b$. The dynamical evolution with $u < v_b$ should be derived by $E_s = E_k$, available at large radii but not relevant here.

For a strong shock, the shock velocity is $v_s \simeq u$. As the SN shock propagates to the point where the radiation diffusive velocity becomes larger than the shock velocity, the radiation escapes from the shock and produces a shock breakout flash. This happens when the optical depth of the material ahead of the shock is $\tau_{br} = c/v_s$ [27]. If the wind is dense enough the shock breakout happens in the wind. The optical depth of wind at radius R is given by $\tau_w = (\rho/m_p)\sigma_T R$. Equating $\tau_w = \tau_{br}$ gives the breakout radius and velocity relation $R_{br} = (A\sigma_T/m_p)v_{br}/c$, which, combined with eq (2), further gives $v_{br} = \left(\frac{E_k v_b^6 m_p c}{4\pi \sigma_T A^2} \right)^{1/9} = 1.1 \times 10^9 \frac{\mathcal{E}^{4/9}}{A_*^{2/9} \mathcal{M}^{1/3}} \text{ cm s}^{-1}$ and then $R_{br} = 2.2 \times 10^{13} \frac{A_*^{7/9} \mathcal{E}^{4/9}}{\mathcal{M}^{1/3}} \text{ cm}$. If the wind optical depth is smaller than τ_{br} , the shock breakout occurs in the stellar surface.

III. PARTICLE ACCELERATION AND ENERGY LOSS

Initially the SN shock is radiation-mediated inside the stellar envelope. Once the radiation escapes, or even before that [10, 28], the shock can no longer be mediated by radiation. Since ion plasma frequency is many orders of magnitude larger than the other relevant frequencies, the shock is expected to become collisionless, and be mediated by collective plasma instabilities [8]. The collisionless shock starts to accelerate particles via diffusive shock acceleration (DSA) [29].

Normalizing the diffusion coefficient to the Bohm value, the acceleration timescale of protons with energy E_p can be given by $t_{acc} = f_B E_p c / v_s^2 e B$, where $f_B \gtrsim 1$ is a constant accounting for the uncertainty of particle diffusion, and $B = \sqrt{8\pi \epsilon_B \rho v_s^2}$ is the postshock magnetic field strength, with ϵ_B being the fraction of energy carried by magnetic field. We take $\epsilon_B = 10^{-2} \epsilon_{B,-2}$ as the typical value, as estimated by X-ray filaments in young SNRs [30, 31]. As for the uncertainty of diffusion, some X-ray observations of young SNRs already indicate fast acceleration close to Bohm limit [31, 32], i.e., $f_B \sim \text{few}$.

In the case of dense stellar winds considered here, the high energy protons will lose energy mainly by pp interactions with background medium, producing pions. The pp energy loss timescale is $t_{pp} = [0.5(\rho_s/m_p)\sigma_{pp}c]^{-1}$, where $\rho_s = 4\rho$ is the postshock density, and the pp pion production cross section is $\sigma_{pp}(E_p) = 3.43 \times 10^{-26} \theta(E_p) \text{ cm}^2$, with $\theta(E_p) = 1 + 0.055l + 0.0073l^2$ and $l = \ln(E_p/1 \text{ TeV})$ [33]. The pp energy loss timescale $t_{pp} \propto R^2/\theta(E_p)$ weakly depends on E_p due to $\theta(E_p)$, and increases with R faster than the dynamical timescale $R/v_s \propto R^{9/8}$.

The particle acceleration suffers from both limited shock expansion time and the energy loss. If the maximum energy of accelerated protons is limited by pp energy loss, by equating $t_{acc} = t_{pp}$, we have the maximum energy

$$E_{p,\max}^{pp}(R) = 35 \frac{\mathcal{E}^{3/2} \epsilon_{B,-2}^{1/2}}{A_*^{7/8} \mathcal{M}^{9/8} f_B} R_{15}^{5/8} \text{ PeV} \quad (3)$$

where $R = 10^{15} R_{15} \text{ cm}$. If limited by the dynamical time of the shock, then $t_{acc} = R/v_s$ gives

$$E_{p,\max}^{dyn}(R) = 94 \frac{A_*^{1/4} \mathcal{E} \epsilon_{B,-2}^{1/2}}{\mathcal{M}^{3/4} f_B} R_{15}^{-1/4} \text{ PeV}. \quad (4)$$

At radius R , the maximum proton energy should be $E_{p,\max}(R) = \min(E_{p,\max}^{pp}, E_{p,\max}^{dyn})$. Since $E_{p,\max}^{pp}$ increases with R but $E_{p,\max}^{dyn}$ decreases, pp energy loss is more important constraint at small radii, but the dynamical time limit more important at large radii. A highest value of $E_{p,\max}(R)$ appears if $E_{p,\max}^{pp} = E_{p,\max}^{dyn}$ (i.e., $t_{acc} = t_{pp} = R/v_s$), which reads

$$E_{p,\max} \theta^{2/7}(E_{p,\max}) = 71 \frac{\mathcal{E}^{8/7} \epsilon_{B,-2}^{1/2}}{A_*^{1/14} \mathcal{M}^{6/7} f_B} \text{ PeV}, \quad (5)$$

insensitive of A and ϵ_B . Note, this is available if the wind is not confined but extends to large distance. However, if the wind is confined to $R_w \approx 10^{15}$ cm, the highest proton energy is determined by eq (3), $E_{p,\max}\theta \sim 35f_B^{-1}$ PeV. So, the proton energy could reach $\lesssim 100$ PeV, for fast particle acceleration, $f_B \sim \text{few}$.

Since the energy loss rate (t_{pp}^{-1}) increases with the proton energy, for a certain R there should be a critical proton energy $E_{p,\text{loss}}(R)$, above which protons significantly lose energy by pp interactions. This can be defined by requiring $t_{pp}(E_{p,\text{loss}}, R) = R/v_s(R)$. Since the work concerns mainly about efficient neutrino production, we are more interested in small radii. At small radii where the maximum proton energy is constrained by pp energy loss rather than the dynamical time, we have $t_{pp}(E_{p,\max}^{pp}) < t_{dyn}$. Since $t_{pp}(E_{p,\text{loss}}) = t_{dyn}$ as defined, we have $t_{pp}(E_{p,\max}^{pp}) < t_{pp}(E_{p,\text{loss}})$, and hence $E_{p,\text{loss}}(R) < E_{p,\max}^{pp}(R)$.

On the other hand, equivalently, we can define by $t_{pp} = R/v_s$ a critical radius for a certain E_p ,

$$R_{pp}(E_p) = 3.1 \times 10^{15} \frac{A_*^{9/7} \mathcal{M}^{3/7} \theta^{8/7}}{\mathcal{E}^{4/7}} \text{cm}, \quad (6)$$

within which the proton can lose energy efficiently by pp interactions. R_{pp} weakly increases with E_p due to function $\theta(E_p)$, so higher energy protons can efficiently lose energy at somewhat larger radii of lower wind density. Since $\theta > 1$, $R_{pp}(E_p) > 3.1 \times 10^{15}$ cm; at $R < 3.1 \times 10^{15}$ cm, all accelerated protons lose energy efficiently by pp interactions.

For protons to be accelerated and lose energy efficiently by pp interactions, it is required that R_{pp} is larger than the shock breakout radius, which is R_{br} if breakout from the wind, or about the stellar radius R_* if breakout from the stellar surface, thus $R_{pp}(E_p) > \max(R_{br}, R_*)$, which reads $A_* > \max\left(6 \times 10^{-5} \frac{\mathcal{E}^2}{\mathcal{M}^{3/2} \theta^{9/4}}, 0.03 \frac{\mathcal{E}^{4/9} R_{*,500}^{7/9}}{\mathcal{M}^{1/3} \theta^{8/9}}\right)$, where we take $R_* = 500 R_{*,500} R_\odot$ as typical value for RSGs. This requirement for A is easily satisfied in the case of the dense wind in SN 2013fs.

IV. NEUTRINO PRODUCTION

A. Individual SNe

It is assumed that in a strong shock the particles are accelerated to follow a flat energy distribution, $dN_p/dE_p \propto E_p^{-s}$ ($E_{p,\min} < E_p < E_{p,\max}$) with $s \approx 2$, which is theoretically predicted and consistent with observed nonthermal emission from SNR shocks [29]. The accelerated particles can carry a fraction $\xi \gtrsim$ tens percents of the shock energy for efficient particle acceleration in the latest DSA theories, whereas $\xi \sim 0.1$ is required for explanation of the origin of Galactic CRs by SNRs [e.g., 12, 34]. We here conservatively take $\xi = 10^{-1} \xi_{-1}$. When the shock propagates to radius R with velocity $v_s(R)$, the shock

energy is $E_{ej}(> v)|_{v=v_s(R)}$, thus the energy distribution of all accelerated protons is given by

$$E_p^2 \frac{dN_p}{dE_p} = \frac{\xi E_{ej}(> v)|_{v=v_s(R)}}{\ln(E_{p,\max}(R)/E_{p,\min})}. \quad (7)$$

Since $E_{p,\max}(R)$ and $E_{p,\min}$ do not change significantly with R , we simply take $1/\ln(E_{p,\max}(R)/E_{p,\min}) \sim 1/7 \ln(10)$. Protons with energy in the range of $E_{p,\text{loss}}(R) < E_p < E_{p,\max}(R)$ essentially lose all their energy by pion production, then the charged pion decays lead to neutrino production. We assume the neutrino flavor ratio after mixing in propagation is $\nu_e : \nu_\mu : \nu_\tau \approx 1 : 1 : 1$. The spectrum of produced neutrinos (per flavor) is

$$E_\nu^2 \frac{dN_\nu}{dE_\nu} = \frac{1}{6} E_p^2 \frac{dN_p}{dE_p} \quad (8)$$

where the factor $1/6$ results from the facts that a fraction of $2/3$ of the proton energy goes to charged pions in pp interactions (i.e., $\pi^+ : \pi^- : \pi^0 \approx 1 : 1 : 1$), and that each neutrino carries a fraction $1/4$ of the charged pion energy. Moreover, in each pp interaction the produced charged pion energy is approximately a factor $1/5$ of the primary proton energy, thus the produced neutrino energy is about $E_\nu \approx E_p/20$.

We consider two cases of the stellar wind: one is extended wind (EW) to radius $R_{pp}(E_{p,\max}) \sim 6 \times 10^{15}$ cm, and another is confined wind (CW) only up to radius $R_w \approx 10^{15} R_{w,15}$ cm. In the EW case, during the whole wind breakout event, the neutrino emission at E_ν is dominated by protons of $E_p = 20E_\nu$ that are accelerated at radius $R = R_{pp}(E_p = 20E_\nu)$. This is because at larger radii where the shock velocity is smaller the shock obtains larger energy from the slower SN ejecta shell. But the radius is limited to $R \lesssim R_{pp}(E_p)$, since at even larger radii the proton energy loss is negligible. Thus, substituting $R = R_{pp}(E_p)$ (eq.6) into eqs. (2) and then (1), one obtains the fraction of shock energy in the bulk ejecta energy, $\eta^{\text{EW}} \equiv E_{ej}(> v)|_{v=v_s(R_{pp})}/E_k = [v_s(R_{pp})/v_b]^{-6}$, i.e.,

$$\eta^{\text{EW}} = 2.1 \times 10^{-2} \frac{A_*^{12/7} \theta^{6/7}}{\mathcal{E}^{3/7} \mathcal{M}^{3/7}}. \quad (9)$$

In the CW case, all accelerated protons significantly lose energy within R_w , thus $\eta^{\text{CW}} \equiv E_{ej}(> v)|_{v=v_s(R_w)}/E_k = [v_s(R_w)/v_b]^{-6}$, i.e.,

$$\eta^{\text{CW}} = 0.91 \times 10^{-2} \frac{A_*^{3/4} R_{w,15}^{3/4}}{\mathcal{M}^{3/4}}. \quad (10)$$

For EW case, plugging ηE_k into eq. (7) and with help of eq. (8), the emitted neutrino spectrum (time-

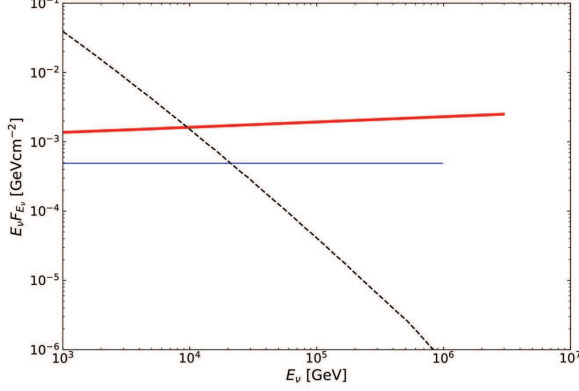


FIG. 1. The neutrino fluence (per flavor) as function of neutrino energy for a SN II at $d_L = 10$ Mpc. The thin (blue) and thick (red) solid lines are the confined-wind (CW) and extended-wind (EW) cases, respectively. The microphysical parameters assumed are $\xi_{-1} = \epsilon_{B,-2} = f_B = 1$. The dashed line is the atmospheric μ neutrino background averaged over zenith angles within 1 degree [35] and integrated over 50 days.

integrated) can be given by[†]

$$E_\nu^2 \frac{dN_\nu}{dE_\nu} = 2.2 \times 10^{46} \frac{\xi_{-1} A_\star^{12/7} \mathcal{E}^{4/7} \theta^{6/7}}{\mathcal{M}^{3/7}} \text{erg}. \quad (\text{EW}) \quad (11)$$

This spectrum weakly depends on E_ν through $\theta(20E_\nu)$, and extends to a cutoff neutrino energy, corresponding to the maximum proton energy, $E_{\nu,\text{max}} = E_{p,\text{max}}/20$. By eq.(5) we have $E_{\nu,\text{max}} \theta^{2/7}(20E_{\nu,\text{max}}) \approx 3.5$ PeV. For CW case similarly we obtain

$$E_\nu^2 \frac{dN_\nu}{dE_\nu} = 9.4 \times 10^{45} \frac{\xi_{-1} A_\star^{3/4} \mathcal{E} R_{w,15}^{3/4}}{\mathcal{M}^{3/4}} \text{erg}, \quad (\text{CW}) \quad (12)$$

independent of E_ν , and $E_{\nu,\text{max}} \theta(20E_{\nu,\text{max}}) \approx 1.8$ PeV (eq.3). Fig 1 shows, for a SN with luminosity distance of $d_L = 10$ Mpc, the spectrum of the neutrino fluence, i.e. the flux integrated over the whole duration, $E_\nu F_{E_\nu} = (E_\nu^2 dN_\nu/dE_\nu)/4\pi d_L^2$.

The duration of neutrino emission can be estimated by $T \simeq \int_0^{R_{pp}} dR/v_s = (8/9)R_{pp}/v_s(R_{pp})$ for EW case, i.e.,

$$T \simeq 52 \frac{A_\star^{11/7} \mathcal{M}^{6/7} \theta^{9/7}}{\mathcal{E}^{8/7}} \text{day}. \quad (\text{EW}) \quad (13)$$

Replacing R_{pp} with R_w we have for CW case,

$$T \simeq 46 \frac{A_\star^{79/56} \mathcal{M}^{45/56} R_{w,15}^{1/8} \theta^{8/7}}{\mathcal{E}^{15/14}} \text{day}. \quad (\text{CW}) \quad (14)$$

[†] The result is comparable to that by [26] for single SN II-P, although the details of two models are different, e.g., different shock dynamics adopted.

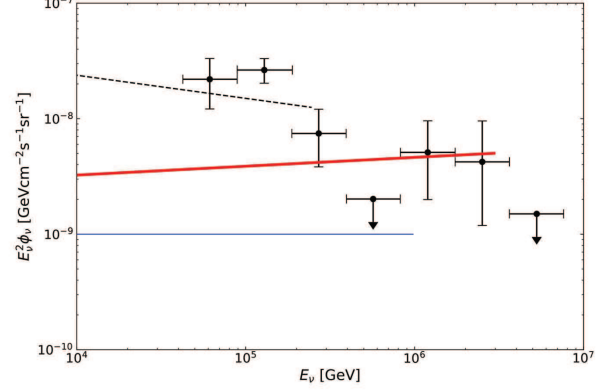


FIG. 2. The diffuse neutrino intensity (per flavor) as function of neutrino energy. The solid lines are the contribution from wind breakouts of SNe II for confined-wind (CW; thin and blue) and extended-wind (EW; thick and red) cases, respectively. The dashed line is the contribution from SNR shock-produced CRs propagating and efficiently losing energy in host galaxies. The data show the latest results of IceCube's high energy starting events [24].

B. Diffuse emission

The diffuse neutrino intensity from all SNe II in the universe can be calculated by integration over the SN rate history, and given by $E_\nu^2 \phi_\nu = \frac{c}{4\pi} \zeta \dot{\rho} t_H E_\nu^2 \frac{dN_\nu}{dE_\nu}$ where t_H is the Hubble timescale, $\dot{\rho}$ is the volumetric rate of local SNe, and ζ accounts for the effect of SN rate density evolution with redshift z . The core-collapse SN rate should follow the star formation rate (SFR), in which case the factor is calculated to be about $\zeta \simeq 3$ [36]. The volumetric rates of nearby core-collapse SNe had been measured, $\dot{\rho} = 0.7 \times 10^{-4} \text{Mpc}^{-3} \text{yr}^{-1}$ [37], most of which are SNe II. Using $t_H = 10$ Gyr, and with help of eqs. (11) or (12), the diffuse neutrino intensity is given by

$$E_\nu^2 \phi_\nu = 2.3 \times 10^{-9} \frac{\xi_{-1} A_\star^{12/7} \mathcal{E}^{4/7} \theta^{6/7}}{\mathcal{M}^{3/7}} \text{GeV cm}^{-2} \text{s}^{-1} \text{sr}^{-1} \quad (\text{EW}) \quad (15)$$

or

$$E_\nu^2 \phi_\nu = 1.0 \times 10^{-9} \frac{\xi_{-1} A_\star^{3/4} \mathcal{E} R_{w,15}^{3/4}}{\mathcal{M}^{3/4}} \text{GeV cm}^{-2} \text{s}^{-1} \text{sr}^{-1}, \quad (\text{CW}) \quad (16)$$

extending up to the neutrino maximum energy, $E_{\nu,\text{max}}$. In CW case the neutrino flux at PeV is about a fraction $\sim 1/3$ of the IceCube detected one, whereas the EW case can well match the IceCube data at $E_\nu \gtrsim 300$ TeV, as shown in Fig 2.

We take a flat CR spectrum in the SN shocks, which is predicted by DSA theory for strong shocks in the test particle assumption, but the theory is with uncertainty. A harder (softer) CR spectrum will enhance (reduce) the neutrino flux at the high energy end. For example, for

a spectral index of $s > 2$, the neutrino flux is lower by a factor of $(20E_\nu/E_{p,\min})^{p-2}/(p-2)\ln(E_{p,\max}/E_{p,\min})$ compared with the case of $s = 2$. For $s \approx 2.2$, this factor is ~ 5 for neutrino flux at $E_\nu \gtrsim 300$ TeV.

V. LOW ENERGY NEUTRINOS FROM CR PROPAGATION

The relatively larger neutrino flux at $E_\nu \lesssim 100$ TeV from the latest IceCube data seems difficult to be accounted for by wind breakouts of SNe II. Here we show that the low energy flux can be naturally explained by the contribution of the SN shocks after wind breakouts. The shock eventually will go through the wind and be driven into the wind bubble or the interstellar medium (ISM). In the late time the SNR shock continues accelerating particles, which, after escape from the shock, interact with the ISM during propagation in the host galaxy. The star formation is dominated by starburst galaxies (SBGs) in the whole star formation history, thus most core-collapse SNe also occur in SBGs, where the relatively larger density and stronger magnetic field in the ISM, compared to normal galaxies, make them strong candidates of neutrino producers [38].

Here we follow Refs. [18, 39] to estimate the low energy neutrino flux. Fermi-LAT had detected GeV gamma-rays from several nearby SBGs, and showed that the ratio of gamma-ray luminosity to SFR for individual SBGs is constant. Applying this constant to all SBGs in the universe, and using the measured SFR evolution with redshift, we can calculate the total GeV gamma-ray flux from all SBGs in the universe. By the correlation between gamma-ray and neutrino production in pp interactions, we can derive the diffuse neutrino intensity at $E_\nu = 0.5$ GeV, $E_\nu^2\phi_\nu = 1.7 \times 10^{-7}(\zeta/3)\text{GeV cm}^{-2}\text{s}^{-1}\text{sr}^{-1}$ [18]. Extrapolating this flux with a power law to higher energy, we have

$$E_\nu^2\phi_\nu \approx 1.5 \times 10^{-8} \zeta \frac{1}{3} (E_\nu/100\text{TeV})^{-0.2} \text{GeV cm}^{-2}\text{s}^{-1}\text{sr}^{-1}. \quad (17)$$

Here a neutrino spectrum of $dN_\nu/dE_\nu \propto E_\nu^{-2.2}$ is assumed, consistent with measured GeV-TeV gamma-ray spectra of the nearby SBGs [40, 41].

The maximum proton energy produced by SNR shock corresponds to the deceleration radius where the shock swept-up medium mass is comparable to the ejecta mass and the shock starts to decelerate significantly. With the SNR shock dynamics, $E_k \simeq (4/3)\pi R^3 n m_p v_s^2$, and equating the acceleration time and dynamical time at the deceleration radius, one obtains a limit to the energy of protons produced by the SNR shock during its whole evolution, $E_p \lesssim 5 \frac{\epsilon_{B,-2}^{1/2} n^{1/6}}{\mathcal{M}^{2/3} f_B} \text{PeV}$, where $n = 10^{-1} n_{-1} \text{cm}^{-3}$ is the medium density for the SNR shock. This limit leads to a spectral cutoff at $E_\nu \simeq 250$ TeV in the neutrino spectrum (eq.17). As shown in Fig 2, the contribution by SNR shock-produced CRs can reasonably account for

the IceCube data at $E_\nu \lesssim 300$ TeV.

Recently there seems to be a tension between the SBG model of neutrino origin and the Fermi-measured extragalactic gamma-ray background (EGB), because the accompanying pp -induced gamma-ray emission should satisfy the EGB measurement. Our model predicts a neutrino flux of $\sim 10^{-8} \text{GeV cm}^{-2}\text{s}^{-1}\text{sr}^{-1}$ with a flat spectrum, $dN_\nu/dE_\nu \propto E_\nu^{-2.2}$ (see Eq.17), which is indeed consistent with the Fermi-measured isotropic gamma-ray background (IGB), i.e. the EGB with resolved point sources subtracted [42]. See, however, e.g., [43], a tension may rise if the non-blazar originated EGB is constrained to be less than a half of the IGB in the range of 50 GeV–1 TeV.

VI. CONCLUSION AND DISCUSSION

According to the recent results that the progenitor stars of SNe II may be commonly surrounded with dense winds ejected by themselves, we investigate the neutrino emission when the SN shocks breakout from winds. We find that the wind breakouts of SN II shocks can convert a fraction $\eta\xi \sim 10^{-3}\xi_{-1}$ of the bulk kinetic energy into neutrinos, and can account for a significant fraction, $\sim 1/3$, of the IceCube neutrinos at $\gtrsim 300$ TeV, if assuming a SN 2013fs-like, confined wind. If the wind extends to $R > R_{pp}(E_{p,\max}) \sim 6 \times 10^{15} \text{cm}$ (EW case), or the CR acceleration in the SN shock is more efficient, $\xi \sim 0.3$, the neutrino flux and spectrum can well fit the IceCube data at $\gtrsim 300$ TeV. Furthermore, the IceCube neutrinos below few hundreds TeV can be explained by SNR shock-produced CRs in SBGs. In this picture, the high energy neutrinos above a few hundreds TeV are contributed by transients of ~ 50 days, whereas the low energy neutrinos below few hundreds TeV are produced in a more steady process.

A subset of SNe II, SNe II_n, have even denser and more extended circumstellar material. They are expected to convert a larger fraction of CR energy into neutrinos, so although they are a small subset, their contribution to the diffuse neutrino flux could be $\sim 10^{-9} \text{GeV cm}^{-2}\text{s}^{-1}\text{sr}^{-1}$ [9], comparable to the regular SNe II. Thus the total contribution from both regular SNe II (CW case) and SNe II_n may account for the IceCube diffuse neutrino flux at $\gtrsim 300$ TeV.

One may worry whether the model satisfies the observational limits on neutrino doublets by IceCube. No neutrino doublet detected in the 4-yr IceCube data sets limits on the source luminosity and density, i.e., $E_\nu L_{E_\nu} \lesssim 10^{42} \text{erg s}^{-1}$ and $n_0 \gtrsim 10^{-7} \text{Mpc}^{-3}$, respectively [20]. In our model, the $\gtrsim 300$ TeV neutrinos are from transient SNe II. During the observational period $\tau = 4$ yrs, the number of SNe II that explode is $\dot{\rho}\tau \sim 3 \times 10^{-3} \text{Mpc}^{-3}$, and the luminosity averaged over the period τ is $\tau^{-1} E_\nu^2 dN_\nu/dE_\nu \sim 10^{38} \text{erg s}^{-1}$. Both are well within the constraints by current IceCube data.

The neutrino luminosity of an individual SN event is,

for confined wind case, $E_\nu L_{E_\nu} \approx E_\nu^2(dN_\nu/dE_\nu)/T \approx 2.4 \times 10^{39} R_{w,15}^{5/8} \theta^{-8/7} (20E_\nu) \text{erg s}^{-1}$. For a SN 10 Mpc away, the observed flux will be $2 \times 10^{-13} \text{erg cm}^{-2} \text{s}^{-1}$, which might be detectable for future 10-Giga ton project Gen2 [44]. Moreover, the accompanying gamma-ray flux from neutral pion decay is related to the neutrino flux as $E_\gamma^2 \Phi_\gamma = 2E_\nu^2 \Phi_\nu(E_\gamma/2) \sim 4 \times 10^{-13} \text{erg cm}^{-2} \text{s}^{-1}$. The south CTA sensitivity is expected to be $\sim 4 \times 10^{-14} \text{erg cm}^{-2} \text{s}^{-1}$ for 50 hr exposure time at 3-10 TeV range. The LHAASO sensitivity at 100 TeV for 1-yr exposure time is similar [45]. Due to background free at $\gtrsim 100$ TeV for LHAASO, we can use scaling of $\propto 1/T$ to estimate the sensitivity for exposure time T , which is $\sim 3 \times 10^{-13} (T/50 \text{day})^{-1} \text{erg cm}^{-2} \text{s}^{-1}$. So both CTA and LHAASO might be able to marginally detect a 10-Mpc event. The expected SN event rate within 10 Mpc is ~ 3 in 10 yrs. A follow-up observation by CTA or LHAASO for the core-collapse SNe within ~ 10 Mpc is encouraging.

It should be noted that the accompanying high-energy gamma-rays may suffer pair-production absorption before escaping from the SN, and hence cannot be observed. We estimate the pair-production optical depth here. The main target photons for $\gamma\gamma$ interactions would be the thermal photons from the photosphere of the SN ejecta. The photon number density at radius R is roughly $n_{ph} \sim L_{SN}/4\pi R^2(3kT)c$, with L_{SN} the bolometric luminosity of the SN thermal radiation, and T the temperature of the thermal radiation. For high-energy photons with E_γ , the threshold photon energy for pair-productions is $E_{th} \sim 2(m_e c^2)^2/E_\gamma$. Thus the pair-production optical

depth for E_γ at R is $\tau_{\gamma\gamma} \sim n_{ph}(\sigma_T/5)R(E_{th}/3kT)$ in the case of $3kT > E_{th}$. Typically $L_{SN} \sim 10^{42} \text{erg s}^{-1}$, and $T \sim 10^4$ K, thus we have $\tau_{\gamma\gamma} \sim 1.6 R_{15}^{-1} (E_\gamma/10 \text{TeV})^{-1}$, which implies that typically $E_\gamma \gtrsim 10$ TeV photons may escape partially. Moreover, the pair-production mean free path for high-energy photons propagating in the extragalactic background lights is $\lambda_{\gamma\gamma} \lesssim 20$ Mpc for $E_\gamma \gtrsim 10$ TeV [see, e.g., 46]. In brief, the 10 – 100 TeV photons accompanying the high-energy neutrinos from SNe II wind breakout events may be able to arrive the Earth avoiding significant absorption either in the sources or in propagation.

NOTES ADDED

First, the very recent finding of delayed shock breakouts shows further evidences that most SNe II have dense circumstellar material [47], supporting our assumption.

Second, very recently a neutrino event IceCube-170922A is claimed to be associated with a blazar TXS 0506+056, with a significance at 3σ level [48]. But more observations are needed to confirm this neutrino-blazar association for most extragalactic neutrinos.

ACKNOWLEDGMENTS

The author thanks Tian-Qi Huang and B.Theodore Zhang for helps in preparation, Kai Wang for discussion, and the several anonymous referees for helpful comments. This work is supported by the NSFC (No. 11773003) and the 973 Program of China (No. 2014CB845800).

-
- [1] E. Waxman and B. Katz, arXiv:1607.01293 [astro-ph.HE].
 - [2] S. Campana *et al.*, Nature **442**, 1008 (2006)
 - [3] A. M. Soderberg *et al.*, Nature **453**, 469 (2008)
 - [4] K. Schawinski *et al.* [SNLS Collaboration], Science **321**, 223 (2008)
 - [5] E. O. Ofek *et al.*, Astrophys. J. **724**, 1396 (2010)
 - [6] S. Gezari *et al.*, Astrophys. J. **804**, no. 1, 28 (2015)
 - [7] P. M. Garnavich, B. E. Tucker, A. Rest, E. J. Shaya, R. P. Olling, D. Kasen and A. Villar, Astrophys. J. **820**, 23 (2016)
 - [8] E. Waxman and A. Loeb, Phys. Rev. Lett. **87**, 071101 (2001)
 - [9] K. Murase, T. A. Thompson, B. C. Lacki and J. F. Beacom, Phys. Rev. D **84**, 043003 (2011)
 - [10] B. Katz, N. Sapir and E. Waxman, arXiv:1106.1898 [astro-ph.HE].
 - [11] K. Kashiyama, K. Murase, S. Horiuchi, S. Gao and P. Meszaros, Astrophys. J. **769**, L6 (2013)
 - [12] V. N. Zirakashvili and V. S. Ptuskin, Astropart. Phys. **78**, 28 (2016)
 - [13] M. Petropoulou, S. Coenders, G. Vasilopoulos, A. Kamble and L. Sironi, Mon. Not. Roy. Astron. Soc. **470**, no. 2, 1881 (2017)
 - [14] O. Yaron *et al.*, Nature Phys. **13**, 510 (2017)
 - [15] M. G. Aartsen *et al.* [IceCube Collaboration], Phys. Rev. Lett. **111**, 021103 (2013)
 - [16] M. G. Aartsen *et al.* [IceCube Collaboration], Science **342**, 1242856 (2013)
 - [17] M. G. Aartsen *et al.* [IceCube Collaboration], Astrophys. J. **835**, no. 2, 151 (2017)
 - [18] B. Wang, X. H. Zhao and Z. Li, JCAP **1411**, no. 11, 028 (2014)
 - [19] B. Wang and Z. Li, Sci. China Phys. Mech. Astron. **59**, no. 1, 619502 (2016)
 - [20] K. Murase and E. Waxman, Phys. Rev. D **94**, no. 10, 103006 (2016)
 - [21] B. T. Zhang and Z. Li, JCAP **1703**, no. 03, 024 (2017)
 - [22] M. G. Aartsen *et al.* [IceCube Collaboration], Astrophys. J. **835**, no. 1, 45 (2017)
 - [23] M. G. Aartsen *et al.* [IceCube Collaboration], Astrophys. J. **843**, no. 2, 112 (2017)
 - [24] M. G. Aartsen *et al.* [IceCube Collaboration], arXiv:1710.01191 [astro-ph.HE].
 - [25] M. G. Aartsen *et al.* [IceCube Collaboration], Astrophys. J. **833**, no. 1, 3 (2016)
 - [26] K. Murase, arXiv:1705.04750 [astro-ph.HE].
 - [27] C. D. Matzner and C. F. McKee, Astrophys. J. **510**, 379 (1999)

- [28] G. Giacinti and A. R. Bell, *Mon. Not. Roy. Astron. Soc.* **449**, no. 4, 3693 (2015)
- [29] R. Blandford and D. Eichler, *Phys. Rept.* **154**, 1 (1987).
- [30] H. J. Volk, E. G. Berezhko and L. T. Ksenofontov, *Astron. Astrophys.* **433**, 229 (2005)
- [31] Y. Uchiyama, F. A. Aharonian, T. Tanaka, T. Takahashi and Y. Maeda, *Nature* **449**, 576 (2007).
- [32] W. Wang and Z. Li, *Astrophys. J.* **789**, 123 (2014)
- [33] S. R. Kelner, F. A. Aharonian and V. V. Bugayov, *Phys. Rev. D* **74**, 034018 (2006)
- [34] V. S. Ptuskin, V. N. Zirakashvili and E. S. Seo, *Astrophys. J.* **718**, 31 (2010)
- [35] R. Abbasi *et al.* [IceCube Collaboration], *Phys. Rev. D* **83**, 012001 (2011)
- [36] E. Waxman and J. N. Bahcall, *Phys. Rev. D* **59**, 023002 (1999)
- [37] W. Li, R. Chornock, J. Leaman, A. V. Filippenko, D. Poznanski, X. Wang, M. Ganeshalingam and F. Mannucci, *Mon. Not. Roy. Astron. Soc.* **412**, 1473 (2011)
- [38] A. Loeb and E. Waxman, *JCAP* **0605**, 003 (2006)
- [39] B. Katz, E. Waxman, T. Thompson and A. Loeb, arXiv:1311.0287 [astro-ph.HE].
- [40] M. Ackermann *et al.* [Fermi-LAT Collaboration], *Astrophys. J.* **755**, 164 (2012)
- [41] F. K. Peng, X. Y. Wang, R. Y. Liu, Q. W. Tang and J. F. Wang, *Astrophys. J.* **821**, no. 2, L20 (2016)
- [42] K. Murase, M. Ahlers and B. C. Lacki, *Phys. Rev. D* **88**, no. 12, 121301 (2013)
- [43] K. Bechtol, M. Ahlers, M. Di Mauro, M. Ajello and J. Vandenbroucke, *Astrophys. J.* **836**, no. 1, 47 (2017)
- [44] M. Ackermann *et al.* [IceCube Gen2 Collaboration], arXiv:1710.01207 [astro-ph.IM].
- [45] G. Di Sciascio [LHAASO Collaboration], *Nucl. Part. Phys. Proc.* **279-281**, 166 (2016)
- [46] B. Baret and V. Van Elewyck, *Rept. Prog. Phys.* **74**, 046902 (2011)
- [47] F. Förster *et al.*, *Nat. Astron.* **2**, no. 10, 808 (2018)
- [48] M. G. Aartsen *et al.* [IceCube and Fermi-LAT and MAGIC and AGILE and ASAS-SN and HAWC and H.E.S.S. and INTEGRAL and Kanata and Kiso and Kapteyn and Liverpool Telescope and Subaru and Swift NuSTAR and VERITAS and VLA/17B-403 Collaborations], *Science* **361**, no. 6398, eaat1378 (2018)